Void Wave Propagation Phenomena in Two-Phase Flow *(Kern Award Lecture)*

R. T. Lahey, Jr.
Dept. of Chemical Engineering, Rensselaer Polytechnic Institute, Troy, NY 12180

A detailed linear and nonlinear analysis of void wave phenomena in two-phase flow is presented. A state-of-the-art, one-dimensional two-fluid model was used as the basis for this analysis. It is shown that void wave dispersion is strongly influenced by phasic slip. In particular, the smaller the slip the more dispersion occurs. It has also been found that nonlinear wave forms, such as shocks and solitons, may occur. Moreover, the virtual mass force was found to be an important parameter in the modeling of void waves. It is shown that void wave analysis is an excellent means of assessing the closure assumptions used in two-fluid models. It is also implied that carefully taken void wave data are needed for this purpose.

Introduction

Void wave propagation mechanisms in two-phase flow are of great importance. Indeed, many transient and steady-state phenomena are controlled by the propagation of void waves. Examples include, flooding, void shocks, density-wave instabilities, and flow regime transition. Significantly, it has also been found that void waves strongly depend on the closure conditions used in two-fluid models. As a consequence, the comparison of void wave analysis with appropriate data offers an excellent means of model assessment.

This paper focuses on the analysis of void wave phenomena. Readers specifically interested in the effect of density waves on two-phase flow instabilities are referred to previous work (Lahey and Podowski, 1989).

Discussion

Consider the two-fluid conservation equations of two-phase flow. For simplicity, only one-dimensional models will be considered, and consideration will be restricted to bubbly air/water flows, since this is representative of the existing data.

The space-time averaged one-dimensional two-fluid conservation equations for adiabatic air/water flow in a constant area duct are given by (Lahey and Drew, 1989):

Conservation of Mass:

$$\frac{\partial}{\partial t}(\langle\alpha_k\rangle\rho_k)+\frac{\partial}{\partial z}(\langle\alpha_k\rangle\rho_k\langle u_k\rangle_k)=0 \quad (1)$$

Conservation of Momentum:

$$\frac{\partial}{\partial t}(\langle\alpha_k\rangle\rho_k\langle u_k\rangle_k)+\frac{\partial}{\partial z}(\langle\alpha_k\rangle\rho_k\langle u_k\rangle_k^2)$$
$$=-\langle\alpha_k\rangle\frac{\partial p_k}{\partial z}+\Delta p_{ki}\frac{\partial\langle\alpha_k\rangle}{\partial z}-\tau_{k_i}\frac{\partial\langle\alpha_k\rangle}{\partial z}$$
$$+\frac{\partial}{\partial z}[\alpha_k\tau^T_{zz_k}]-\langle\alpha_k\rangle\rho_k g_k\cos\theta+M_{k_i}-\tau_{k_w}/D_H \quad (2)$$

where subscript k denotes either the gas ($k=g$) or the liquid ($k=\ell$) phase. In this work it will be assumed that both phases are incompressible.

To obtain closure, appropriate constitutive equations must be used to model the interaction between the phases. The momentum transfer between the gas and liquid phases can be written (Cheng et al., 1985):

$$M_{\ell_i}=-M_{g_i}=\langle\alpha\rangle[F_D+F_{vm}] \quad (3)$$

where

$$\langle\alpha\rangle\triangleq\langle\alpha_g\rangle. \quad (4)$$

The interfacial drag force, F_D, for bubbly flow of uniform bubble size, R_b, can be modeled as:

$$F_D=\frac{3}{8}\rho_\ell\frac{C_D}{R_b}(\langle u_g\rangle_g-\langle u_\ell\rangle_\ell)\,|\langle u_g\rangle_g-\langle u_\ell\rangle_\ell| \quad (5)$$

The drag coefficient, C_D, depends on the flow regime. For example, for distorted bubbly flows it is given by (Harmathy, 1960):

$$C_D=\frac{4}{3}R_b\left[\frac{g(\rho_\ell-\rho_g)}{\sigma(1-\langle\alpha\rangle)}\right]^{1/2} \quad (6)$$

In contrast, the interfacial drag force can also be written as:

$$F_D=\rho_\ell\frac{f_i}{D_H}(\langle u_g\rangle_g-\langle u_\ell\rangle_\ell)\,|\langle u_g\rangle_g-\langle u_\ell\rangle_\ell| \quad (7)$$

where, for example, the interfacial friction factor for undistorted bubbles is given by (Ishii and Zuber, 1978):

$$f_i=18\frac{D_H}{D_b}\frac{[1+0.1\,Re_{2\phi}^{0.75}]}{Re_{2\phi}} \quad (8a)$$

where

$$Re_{2\phi}=\frac{\rho_\ell(\langle u_g\rangle_g-\langle u_\ell\rangle_\ell)D_b}{\mu_\ell(1-\alpha)^{-2.5(\mu_g+0.4\mu_\ell)/(\mu_g+\mu_\ell)}} \quad (8b)$$

The virtual mass force, F_{VM}, is given by,

$$F_{vm}=\rho_\ell\,C_{vm}\,a_{vm} \quad (9)$$

The virtual volume coefficient, C_{vm}, can be expressed as an empirical function of the global void fraction (Ruggles et al., 1988) as,

$$C_{vm}=0.5\;[1+12\langle\alpha\rangle^2], \qquad (\langle\alpha\rangle)\le 20\% \quad (10)$$

and the virtual mass acceleration, a_{vm}, is given by (Drew and Lahey, 1987):

$$a_{vm}=\left[\frac{\partial\langle u_g\rangle_g}{\partial t}+\langle u_g\rangle_g\frac{\partial\langle u_g\rangle_g}{\partial z}\right]-\left[\frac{\partial\langle u_\ell\rangle_\ell}{\partial z}+\langle u_\ell\rangle_\ell\frac{\partial\langle u_\ell\rangle_\ell}{\partial z}\right] \quad (11a)$$

or equivalently,

$$a_{vm}=\left[\frac{D_g\langle u_g\rangle_g}{Dt}-\frac{D_\ell\langle u_\ell\rangle_\ell}{Dt}\right] \quad (11b)$$

Since, for bubbly flow, the gas phase is assumed to be dispersed within the liquid phase, the wall shear stress on the gas phase is,

$$\tau_{g_w}=0 \quad (12a)$$

while the liquid-phase wall shear stress is,

$$\tau_{\ell_w}=\frac{1}{2}\frac{f_w}{D_H}\rho_\ell\langle u_\ell\rangle_\ell|\langle u_\ell\rangle_\ell| \quad (12b)$$

For low-pressure air/water flows, the interfacial pressure in the gas phase is often related to the average pressure of the gas phase by,

$$\Delta p_{gi}=p_{gi}-p_g\cong 0 \quad (13)$$

This is normally a good assumption and implies that one is dealing with situations in which the bubble has essentially a uniform internal pressure.

In contrast, the difference between the interfacial average pressure and the mean pressure in the liquid phase is, for a nonpulsating bubble, given by (Stuhmiller, 1977):

$$p_{\ell i}-p_\ell=\Delta p_{\ell i}=-\frac{\rho_\ell}{4}(\langle u_g\rangle_g-\langle u_\ell\rangle_\ell)^2 \quad (14)$$

The Reynolds stress ($\underline{\underline{\tau}}_k^T$) is negligible in the gas phase but not in the liquid phase. It is beyond the current state-of-the-art to model this term in general, however, the Reynolds stress in the liquid phase due to bubble-induced turbulence has been given by Nigmatulin (1979) as:

$$\underline{\underline{\tau}}_\ell^T=-\langle\alpha\rangle\rho_\ell[C_1|\langle\underline{u}_g\rangle_g-\langle\underline{u}_\ell\rangle_\ell|^2\underline{\underline{I}}+C_2(\langle\underline{u}_g\rangle_g-\langle\underline{u}_\ell\rangle_\ell)(\langle\underline{u}_g\rangle_g-\langle\underline{u}_\ell\rangle_\ell)] \quad (15a)$$

It can be shown (Biesheuvel and van Wijngaarden, 1984) that for a spherical bubble the coefficients C_1 and C_2 are given by,

$$C_1=\frac{3}{20} \qquad C_2=\frac{1}{20} \quad (15b)$$

It should be noted that for one-dimensional pipe flow, Eqs. 15 reduce to:

$$\tau_{zz_\ell}^T=-\frac{1}{5}\langle\alpha\rangle\rho_\ell(\langle\underline{u}_g\rangle_g-\langle\underline{u}_\ell\rangle_\ell)^2 \quad (16)$$

Hence, the Reynolds stress gradient term in Eq. 2 can be written as,

$$\frac{\partial}{\partial z}\left[(1-\langle\alpha\rangle)\tau_{zz_\ell}^T\right]=-\frac{\partial}{\partial z}\left[\frac{1}{5}\langle\alpha\rangle(1-\langle\alpha\rangle)\rho_\ell(\langle\underline{u}_g\rangle_g-\langle\underline{u}_\ell\rangle_\ell)^2\right] \quad (17)$$

This is the same expression as was developed by Biesheuvel and van Wijngaarden (1984) and used by Pauchon and Banerjee (1988).

The wall-induced interfacial shear, τ_{k_i} is often set to zero. However, in this study it was assumed that $\tau_{g_i}=0$ and $\tau_{\ell_i}=\tau_{zz_\ell}^T$. Interestingly, when this is done the third and fourth terms on the righthand side of Eq. 2 combine to yield,

$$-\tau^T_{zz_k}\frac{\partial\langle\alpha_k\rangle}{\partial z}+\frac{\partial}{\partial z}[\langle\alpha_k\rangle\tau^T_{zz_k}]=\langle\alpha_k\rangle\frac{\partial}{\partial z}[\tau^T_{zz_k}] \quad (18)$$

For the quasi-static conditions that are typical of void wave phenomena, we note from Eq. 14, and the well-known Laplace equation, that:

$$p_g-p_\ell=\frac{2\sigma}{R_b}-\frac{\rho_\ell}{4}(\langle u_g\rangle_g-\langle u_\ell\rangle_\ell)^2 \quad (19)$$

We have now achieved closure. Equations 1-19 comprise a state-of-the-art, one-dimensional two-fluid model that is appropriate for use in the analysis of void waves in bubbly flows. Let us first perform a linear analysis.

Linear Analysis of Void Wave Propagation

Linear void wave propagation phenomena have been extensively studied and have been used for the assessment of two-fluid model constitutive relations (Park et al., 1990; Ruggles et al., 1988; Pauchon and Banerjee, 1988; Bouré, 1988). Moreover, it has been proposed that the void waves may be responsible for flow regime transition (Saiz-Jabardo and Bouré, 1989; Tournaire, 1987). Let us now use the two-fluid model to gain a more in-depth understanding of void wave phenomena, and how void wave propagation is related to the constitutive equations we have used to achieve closure.

It is convenient to use dimensionless forms of Eqs. 1 and 2:

$$\frac{\partial\alpha_k}{\partial t^*}+\frac{\partial}{\partial z^*}(\alpha_k u_k^*)=0 \quad (20)$$

$$\rho_k^*\left[\frac{\partial u_k^*}{\partial t^*}+u_k^*\frac{\partial u_k^*}{\partial z^*}\right]=-\frac{\partial p_k^*}{\partial z^*}+\frac{\Delta p^*_{k_i}}{\alpha_k}\frac{\partial\alpha_k}{\partial z^*}-\frac{\tau^*_{k_i}}{\alpha_k}\frac{\partial\alpha_k}{\partial z^*}$$
$$+\frac{1}{\alpha_k}\frac{\partial}{\partial z^*}(\alpha_k\tau^{T*}_{zz_k})-\rho_k^*\cos\theta+\frac{M^*_{k_i}}{\alpha_k}-\frac{\tau^*_{kw}}{\alpha_k}\frac{4}{Fr_o} \quad (21)$$

where

$$u_k^*=\frac{\langle u_k\rangle_k}{u_{R_o}},\quad t^*=\frac{g}{u_{R_o}}t,\quad z^*=\frac{g}{u^2_{R_o}}z,\quad \alpha_g=\langle\alpha\rangle$$

$$p_k^*=\frac{p_k}{\rho_L u^2_{R_o}},\quad \tau_k^*=\frac{\tau_k}{\rho_L u^2_{R_o}},\quad \rho_k^*=\frac{\rho_k}{\rho_L},\quad \alpha_\ell=1-\langle\alpha\rangle$$

$$M^*_{k_i}=\frac{M_{k_i}}{\rho_L g},\quad Fr_o=\frac{gD_H}{u^2_{R_o}},\quad u_{R_o}=(\langle u_g\rangle_g-\langle u_\ell\rangle_\ell)$$

Let us now first perform a linear analysis of void wave propagation. When the two-phase system is disturbed about a fully developed steady-state condition, the perturbed variables satisfy:

$$\frac{\partial\delta\alpha_k}{\partial t^*}+u^*_{k_o}\frac{\partial\delta\alpha_k}{\partial z^*}+\alpha_{k_o}\frac{\partial\delta u_k^*}{\partial z^*}=0 \quad (22)$$

$$\rho_k^*\left[\frac{\partial\delta u_k^*}{\partial t^*}+u^*_{k_o}\frac{\partial\delta u_k^*}{\partial z^*}\right]=-\frac{\partial\delta p_k^*}{\partial z^*}+\frac{\Delta p^*_{k_{io}}}{\alpha_{k_o}}\frac{\partial\delta\alpha_k}{\partial z^*}-\frac{\tau^*_{k_{io}}}{\alpha_{k_o}}\frac{\partial\delta\alpha_k}{\partial z^*}$$
$$+\frac{\tau^{T*}_{zzk_o}}{\alpha_{k_o}}\frac{\partial\delta\alpha_k}{\partial z^*}+\frac{\partial\delta\tau^{T*}_{zz_k}}{\partial z^*}+\frac{\delta M^*_{k_i}}{\alpha_{k_o}}-\frac{M^*_{k_o}}{\alpha^2_{k_o}}\delta\alpha_k$$
$$-\frac{4}{Fr_o}\left[\frac{\delta\tau^*_{kw}}{\alpha_{k_o}}-\frac{\tau^*_{kw_o}}{\alpha^2_{k_o}}\delta\alpha_k\right] \quad (23)$$

where

$$\delta\alpha_k=\alpha_k-\alpha_{k_o},$$

and similarly for u_ℓ^* and u_g^*.

To achieve closure, the constitutive relations have been expressed in terms of the state variables, u_ℓ^* , u_g^*, and $\alpha=\alpha_g$. Thus, we may assume that the righthand side of Eq. 23 can be expressed as $\delta F^*+\delta F^*_{vm}$, where:

$$\delta F^*=\frac{\partial F^*}{\partial\alpha}\bigg|_o\delta\alpha+\frac{\partial F^*}{\partial u_\ell^*}\bigg|_o\delta u_\ell^*+\frac{\partial F^*}{\partial u_g^*}\bigg|_o\delta u_g^* \quad (24)$$

Equation (24) can only be used for the algebraic interfacial and wall transfer laws. Other forces, such as those due to virtual mass (F^*_{vm}), must be treated differently. Using Eqs. 9 and 11, the nondimensional virtual mass force can be written as:

$$F^*_{vm}=C_{vm}\left[\frac{\partial u_g^*}{\partial t^*}+u_g^*\frac{\partial u_g^*}{\partial z^*}-\frac{\partial u_\ell^*}{\partial t^*}-u_\ell^*\frac{\partial u_\ell^*}{\partial z^*}\right] \quad (25)$$

Assuming C_{vm} is a constant, we obtain the perturbation in the virtual mass force as:

$$\delta F^*_{vm}=C_{vm}\left[\frac{\partial\delta u_g^*}{\partial t^*}+u^*_{g_o}\frac{\partial\delta u_g^*}{\partial z^*}-\frac{\partial\delta u_\ell^*}{\partial t^*}-u^*_{\ell_o}\frac{\partial\delta u_\ell^*}{\partial z^*}\right] \quad (26)$$

If we neglect the interfacial pressure difference for the gas phase (i.e., $\Delta p^*_{g_i}$), and the surface tension between phases is neglected (i.e., $p^*_{g_i}=p^*_{\ell_i}$), we obtain,

$$\delta p_g^*-\delta p_\ell^*=\delta\Delta p^*_{\ell_i} \quad (27)$$

If we subtract Eq. 23 for the gas phase from that for the liquid phase to eliminate pressure, and eliminate gradients in the velocity, and the phase average pressure perturbations by using Eqs. 22 and 24, we obtain:

$$K_1\frac{\partial\delta\alpha}{\partial t^*}+K_2\frac{\partial\delta\alpha}{\partial z^*}+K_3\frac{\partial^2\delta\alpha}{\partial t^{*2}}+K_4\frac{\partial^2\delta\alpha}{\partial t^*\partial z^*}+K_5\frac{\partial^2\delta\alpha}{\partial z^{*2}}=0$$

where

$$K_1 = -\frac{1}{(1-\alpha_o)}\left[\frac{1}{(1-\alpha_o)}\frac{\partial F_D^*}{\partial u_\ell^*}\bigg|_o - \frac{1}{\alpha_o}\frac{\partial F_D^*}{\partial u_g^*}\bigg|_o\right] + \frac{4}{Fr_o}\left\{\frac{1}{(1-\alpha_o)}\left[\frac{1}{(1-\alpha_o)}\frac{\partial \tau_{\ell w}^*}{\partial u_\ell^*}\bigg|_o - \frac{1}{\alpha_o}\frac{\partial \tau_{\ell w}^*}{\partial u_g^*}\bigg|_o\right] - \frac{1}{\alpha_o}\left[\frac{1}{(1-\alpha_o)}\frac{\partial \tau_{gw}^*}{\partial u_\ell^*}\bigg|_o - \frac{1}{\alpha_o}\frac{\partial \tau_{gw}^*}{\partial u_g^*}\bigg|_o\right]\right\} \tag{29}$$

$$K_2 = -\frac{1}{(1-\alpha_o)}\left[\frac{\partial F_D^*}{\partial \alpha}\bigg|_o + \frac{u_{\ell_o}^*}{(1-\alpha_o)}\frac{\partial F_D^*}{\partial u_\ell^*}\bigg|_o - \frac{u_{g_o}^*}{\alpha_o}\frac{\partial F_D^*}{\partial u_g^*}\bigg|_o\right] - \frac{F_{D_o}^*}{(1-\alpha_o)^2} + \frac{4}{Fr_o}\left\{\frac{1}{(1-\alpha_o)}\left[\frac{\partial \tau_{\ell w}^*}{\partial \alpha}\bigg|_o + \frac{u_{\ell_o}^*}{(1-\alpha_o)}\frac{\partial \tau_{\ell w}^*}{\partial u_\ell^*}\bigg|_o - \frac{u_{g_o}^*}{\alpha_o}\frac{\partial \tau_{\ell w}^*}{\partial u_g^*}\bigg|_o\right] - \frac{1}{\alpha_o}\left[\frac{\partial \tau_{gw}^*}{\partial \alpha}\bigg|_o + \frac{u_{\ell_o}^*}{(1-\alpha_o)}\frac{\partial \tau_{gw}^*}{\partial u_\ell^*}\bigg|_o - \frac{u_{g_o}^*}{\alpha_o}\frac{\partial \tau_{gw}^*}{\partial u_g^*}\bigg|_o\right] + \frac{\tau_{\ell w_o}^*}{(1-\alpha_o)^2} + \frac{\tau_{g w_o}^*}{\alpha_o^2}\right\} \tag{30}$$

$$K_3 = \frac{1}{(1-\alpha_o)} + \frac{\rho_g^*}{\alpha_o} + \frac{C_{vm}}{\alpha_o(1-\alpha_o)^2} \tag{31}$$

$$K_4 = -2\left\{\frac{u_{\ell_o}^*}{(1-\alpha_o)} + \rho_g^*\frac{u_{g_o}^*}{\alpha_o} + \frac{C_{vm}}{(1-\alpha_o)}\left[\frac{u_{\ell_o}^*}{(1-\alpha_o)} + \frac{u_{g_o}^*}{\alpha_o}\right]\right\} - \frac{1}{(1-\alpha_o)}\frac{\partial(-\Delta p_{\ell_i}^* - \tau_{zz_\ell}^{T^*} + \tau_{zz_g}^{T^*})}{\partial u_\ell^*} + \frac{1}{\alpha_o}\frac{\partial(-\Delta p_{\ell_i}^* - \tau_{zz_\ell}^{T^*} + \tau_{zz_g}^{T^*})}{\partial u_g^*} \tag{32}$$

$$K_5 = \frac{u_{\ell_o}^{*2}}{(1-\alpha_o)} + \rho_g^*\frac{u_{g_o}^{*2}}{\alpha_o} + \frac{C_{vm}}{(1-\alpha_o)}\left[\frac{u_{\ell_o}^{*2}}{(1-\alpha_o)} + \frac{u_{g_o}^{*2}}{\alpha_o}\right] + \frac{\Delta p_{\ell_{io}}^* - \tau_{\ell_{io}}^* + \tau_{zz_{\ell_o}}^{T^*}}{(1-\alpha_o)} + \frac{-\tau_{g_{io}}^* + \tau_{zz_{g_o}}^{T^*}}{\alpha_o} + \frac{\partial(-\Delta p_{\ell_i}^* - \tau_{zz_\ell}^{T^*} + \tau_{zz_g}^{T^*})}{\partial \alpha}\bigg|_o + \frac{u_{\ell_o}^*}{(1-\alpha_o)}\frac{\partial(-\Delta p_{\ell_i}^* - \tau_{zz_\ell}^{T^*} + \tau_{zz_g}^{T^*})}{\partial u_\ell^*}\bigg|_o - \frac{u_{g_o}^*}{\alpha_o}\frac{\partial(-\Delta p_{\ell_i}^* - \tau_{zz_\ell}^{T^*} + \tau_{zz_g}^{T^*})}{\partial u_g^*}\bigg|_o \tag{33}$$

Equation 28 can be rewritten in more compact form as:

$$\frac{\partial \delta\alpha}{\partial t^*} + a_+^*\frac{\partial \delta\alpha}{\partial z^*} + T^*\left(\frac{\partial}{\partial t^*} + r_-^*\frac{\partial}{\partial z^*}\right) \times \left(\frac{\partial}{\partial t^*} + r_+^*\frac{\partial}{\partial z^*}\right)\delta\alpha = 0 \tag{34}$$

where

$$a_+^* = \frac{a_+}{u_{R_o}} = \frac{K_2}{K_1} \tag{35a}$$

$$T^* = \frac{K_3}{K_1} \tag{35b}$$

$$r_\pm^* = \frac{r_\pm}{u_{R_o}} = -\frac{K_4}{2K_3} \pm \sqrt{\frac{1}{4}\left(\frac{K_4}{K_3}\right)^2 - \left(\frac{K_5}{K_3}\right)} \tag{35c}$$

It can be shown (Whitham, 1974) that a_+^*, $r_\pm^*$, and T^* are the dimensionless forms of the kinematic wave speed, characteristics, and the relaxation time, respectively. It is interesting to note that Eq. 34 is similar to, but more general than, the previous results of Pauchon and Banerjee (1988).

Let us now consider the mathematical properties of Eq. 34. The dispersion relationship can be obtained by assuming a solution of the form:

$$\delta\alpha = \alpha' e^{i(\kappa^* z^* - \omega^* t^*)} \tag{36}$$

Inserting Eq. 36 into Eq. 34, we obtain the following linear dispersion relationship:

$$i(\omega^* - a_+^*\kappa^*) + T^*(\omega^* - r_-^*\kappa^*)(\omega^* - r_+^*\kappa^*) = 0 \tag{37}$$

If we consider the region where Eq. 34 is hyperbolic (i.e., where $r_\pm^*$ are real), the roots of Eq. 37 for traveling waves (where κ^* is real) can be found by solving the following coupled equations:

$$\omega_I^* = \frac{1}{2T^*}\left[\frac{a_+^* - \bar{r}}{C_\alpha^* - \bar{r}} - 1\right] \tag{38a}$$

$$\omega_R^{*2} = \frac{C_\alpha^{*2}}{4T^{*2}}\left[\frac{(a_+^* - \bar{r})^2 - (C_\alpha^* - \bar{r})^2}{(C_\alpha^* - \bar{r})^2(C_\alpha^* - r_-^*)(C_\alpha^* - r_+^*)}\right] \tag{38b}$$

where

$$\omega^* = \omega_R^* + i\omega_I^* \tag{39a}$$

$$C_\alpha^* = \frac{\omega_R^*}{\kappa^*} \tag{39b}$$

$$\bar{r} = \frac{(r_+^* + r_-^*)}{2} \tag{39c}$$

Equations 38b and 39b imply that void wave dispersion is pronounced for large values of the relaxation time (T^*), since the wave speed C_α^* is strongly dependent on angular frequency ω_R^* when relaxation time is large.

It is interesting to plot Eqs. 38 and 39. As shown in Figures 1 and 2, two speeds of void wave propagation are possible (i.e., C_α^+ and C_α^- waves) for a specified angular frequency, ω_R^*. The larger celerity, C_α^+, is easily recognized as the predominant speed of propagation, and, in the limit as $\omega_R \rightarrow 0$

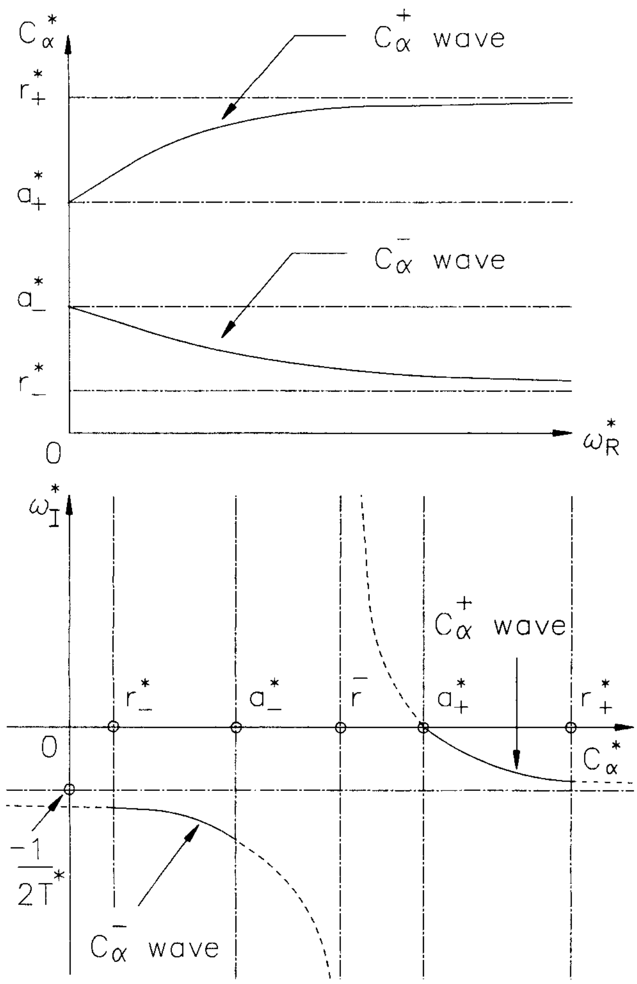

Figure 1. Plot of Eqs. 38 for $r_- < a_+ < r_+$ (stable).

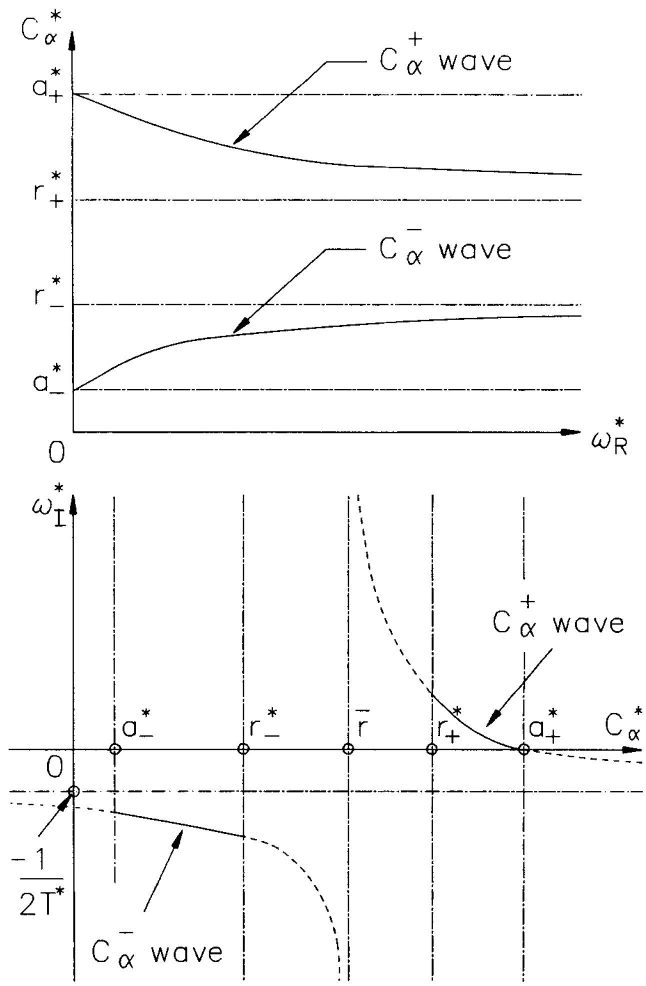

Figure 2. Plot of Eqs. 38 for $a_+ > r_+$ (unstable).

it is the so-called kinematic wave speed a_+ (Wallis, 1969). However, a complementary void wave celerity, (C_α^-) is also present. The dispersion relationship implies that the C_α^- wave is slower than C_α^+ and, as shown in Figures 1 and 2, the complementary void wave has relatively large damping. As a consequence it is not easily measured. The complementary kinematic wave speed, a_-, (i.e., C_α^- at zero frequency), can be found from Eq. 38b) as:

$$\lim_{\omega_R^* \to 0} C_\alpha^{*-} = a_-^* = r_+^* + r_-^* - a_+^* \tag{40}$$

The well-known stability criteria (Whitham, 1974) for C_α^+ waves can easily be seen, by examining the solid lines in Figures 1 and 2, to be:

$$r_-^* < a_+^* < r_+^* \tag{41}$$

Appropriate constitutive relations must be used to quantify the properties of void waves. Using the constitutive relations previously discussed, and taking the low-frequency (ω_R) limit, we obtain the dimensionless form of the kinematic wave speed in a frame referenced to the liquid-phase velocity:

$$A_+^* = \frac{a_+ - \langle u_\ell \rangle_{\ell o}}{u_{R_o}} = 1 - n\alpha_o \tag{42}$$

where

$$n = \frac{\left[\frac{1}{f_{i_o}} \frac{\partial f_i}{\partial u_\ell^*}\bigg|_o - (1-\alpha_o)\frac{1}{f_{i_o}}\frac{\partial f_i}{\partial \alpha}\bigg|_o - 3 - \frac{4(1+\alpha_o)\tau_{\ell w_o}^*}{f_{i_o}} \right]}{\left[\alpha_o \frac{1}{f_{i_o}}\frac{\partial f_i}{\partial u_\ell^*}\bigg|_o - (1-\alpha_o)\frac{1}{f_{i_o}}\frac{\partial f_i}{\partial u_g^*} - 2 - \frac{8\alpha_o}{u_{\ell_o}^*}\frac{\tau_{Lw_o}^*}{f_{i_o}} \right]} \tag{43}$$

Using Eqs. 8 we obtain:

$$n = \frac{2.0 + 2.5\mu_m + (0.275 + 0.0625\mu_m)Re_{2\phi_o}^{0.75} + \left[\frac{(1+\alpha_o)\tau_{\ell w_o}^* D_b}{4.50\, D_H}\right] Re_{2\phi_o}}{1 + 0.1750\, Re_{2\phi_o}^{0.75} + \left[\frac{\alpha_o \tau_{\ell w_o}^* D_b}{2.25\, D_H u_{\ell_o}^*}\right] Re_{2\phi_o}} \tag{44}$$

Similarly, Eq. 35c yields,

$$\lambda_\pm^* \triangleq \frac{r_\pm - \langle u_\ell \rangle_{\ell o}}{u_{R_o}} = V^* \pm \sqrt{\nu^*/\tau^*} \tag{45}$$

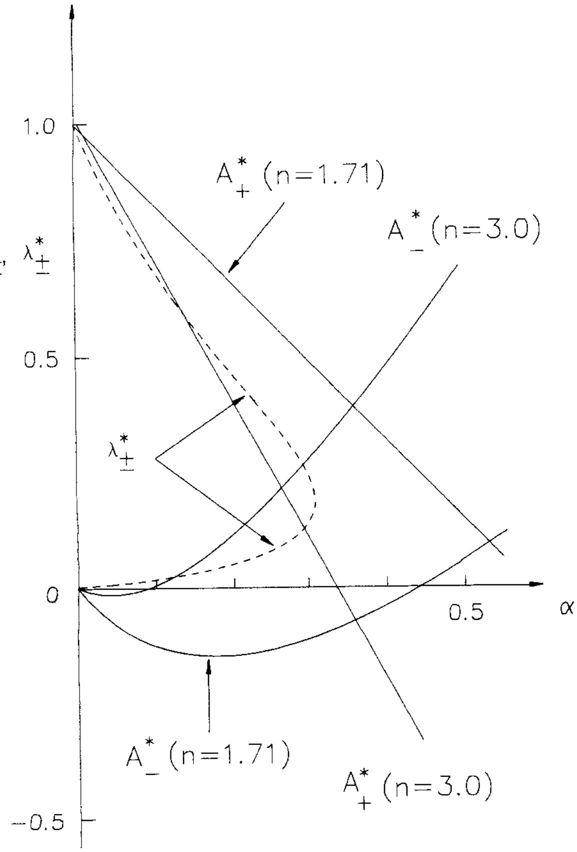

Figure 3. Kinematic wave speeds and characteristics.
C_{vm} = 0.5; η = 0.25; k = 0.2; ρ_g = 0; f_w = 0

where

$$V^* \triangleq \frac{(1-\alpha_o)[C_{vm}-\eta-k\alpha_o+\rho_g^*(1-\alpha_o)]}{\alpha_o(1-\alpha_o)+C_{vm}+\rho_g^*(1-\alpha_o)^2} \quad (46a)$$

$$\tau^* \triangleq \alpha_o(1-\alpha_o)+C_{vm}+\rho_g^*(1-\alpha_o)^2 \quad (46b)$$

$$\nu^* \triangleq (1-\alpha_o)^2 \frac{[C_{vm}-\eta-k\alpha_o+\rho_g^*(1-\alpha_o)]^2}{[\alpha_o(1-\alpha_o)+C_{vm}+\rho_g^*(1-\alpha_o)^2]} + \alpha_o(1-\alpha_o)(\eta+k-C_{vm}) + 2(1-\alpha_o)^2\left(\eta-\frac{C_{vm}}{2}\right) - \rho_g^*(1-\alpha_o)^2 - k\alpha_o^2(1-\alpha_o) \quad (46c)$$

It should be noted that, except for the last term on the righthand side of Eq. 46c, Eqs. 45-46 reduce to the results of Pauchon and Banerjee (1988) if we let: f_w = 0, ρ_g^* = 0, C_{vm} = 1/2, η = 1/4, and k = 1/5. This difference reflects the fact that Pauchon and Banerjee (1988) assumed $\tau_{\ell_i}=0$ in their study rather than letting $\tau_{\ell_i}=\tau^T_{zz_\ell}$ as was done herein.

If we neglect the wall shear stress in Eq. 44, we find that $1.71 \le n < 3.0$ for all values of $Re_{2\phi o}$. To bound the possibilities, the dimensionless kinematic wave speed given by Eq. 42 for n = 1.71 and n = 3.0 is shown in Figure 3 along with the characteristics. According to the stability criteria given by Eq. 41, the kinematic wave is unstable (i.e., it grows during propagation) over a wide range of $Re_{2\phi o}$. We note that, since $Re_{2\phi o}$ is proportional to relative velocity, n is increased as the relative velocity is decreased. Thus, the kinematic wave can be stabilized by reducing the phasic slip in the steady flow. It should be noted that since $Re_{2\phi o}$ is also proportional to the size of bubbles, small bubbles also stabilize the kinematic wave.

The dimensionless relaxation time can be found from Eq. 37 as:

$$T^* = \frac{gT}{u_{R_o}} = \frac{Fr_o Re_{2\phi_o}}{18D_H/D_b} \frac{[\alpha_o(1-\alpha_o)+C_{vm}+\rho_g^*(1-\alpha_o)^2]}{\left[1+0.175\,Re_{2\phi_o}^{0.75}+\left(\alpha_o\tau^*_{tw_o}\frac{D_b}{2.25D_H}\right)Re_{2\phi_o}\right]} \quad (47)$$

As can be seen in Eq. 47, the Froude number $(gD_H/u^2_{R_o})$ strongly influences the void wave relaxation time.

The dispersion relationship presented herein yields a complementary kinematic wave, (a_-). Using the constitutive relations previously discussed and Eq. 40, we find that the dimensionless speed of the complementary kinematic wave is:

$$A^*_- = \frac{a_- - \langle u_\ell\rangle_{\ell o}}{u_{R_o}} = \lambda^*_+ + \lambda^*_- - A^*_+ \quad (48)$$

As shown in Figure 3, the coalescence of kinematic wave speeds (i.e., $A^*_+ = A^*_-$) occurs at a lower void fraction than where the characteristics coalesce ($\lambda^*_+ = \lambda^*_-$) when the corresponding kinematic void wave (a_+) is more stable.

If we use Eqs. 38a and 48, we obtain the temporal damping of the C^-_α wave as,

$$\omega_I = 18\frac{u_{R_o}[1+0.175\,Re_{2\phi_o}^{0.75}+(\alpha_o\tau^*_{tw_o}D_b/2.25D_H)Re_{2\phi_o}]}{D_b[\alpha_o(1-\alpha_o)+C_{vm}+\rho_g^*(1-\alpha_o)^2]Re_{2\phi_o}} \quad (49)$$

This implies that the C^-_α wave has large temporal damping when the phasic slip is large. Thus, based upon the constitutive relations used herein, it appears to be possible to observe the C^-_α wave only when phasic slip is small. Naturally, once C^-_α is known we may determine a_- since, $\lim_{\omega_R \to 0} C^-_\alpha = a_-$.

It is also interesting to relate these results to classical kinematic wave theory. A kinematic drift-flux model for void waves has been proposed by Wallis (1969). Significantly, this model is based entirely on steady-state considerations. The celerity of void perturbations is given by

$$a_+ = \left(\frac{\partial j_g}{\partial\langle\alpha\rangle}\right)_j = j + \frac{\partial j_{g\ell}}{\partial\langle\alpha\rangle} \quad (50)$$

Since

$$j = \langle\alpha\rangle\langle u_g\rangle_g + (1-\langle\alpha\rangle)\langle u_\ell\rangle_\ell$$

we have

$$A^*_+ = \frac{a_+ - \langle u_\ell\rangle_{\ell o}}{u_{R_o}} = \langle\alpha\rangle + \frac{1}{u_{R_o}}\frac{\partial j_{g\ell}}{\partial\langle\alpha\rangle} \quad (51)$$

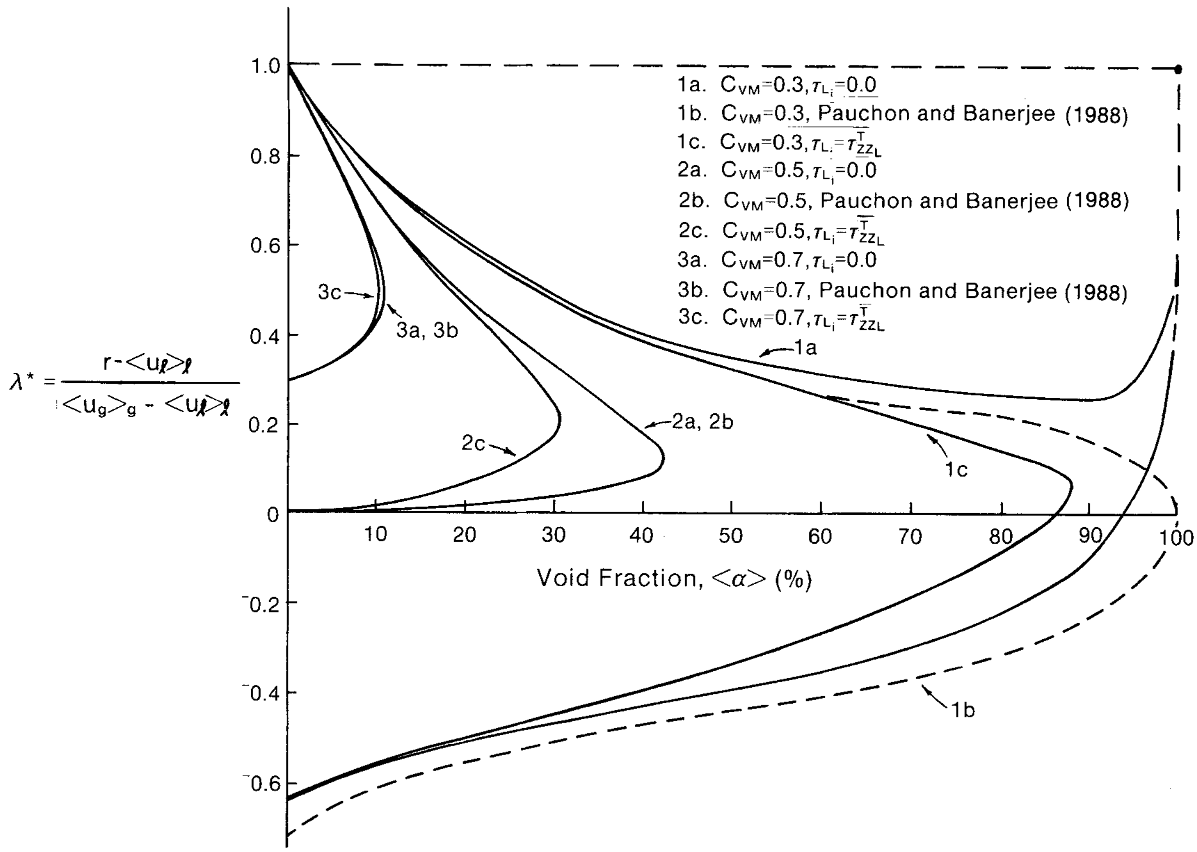

Figure 4. Sensitivity of eigenvalues to changes in C_{vm} (with Reynolds stress).

Wallis (1969) has also proposed an empirical drift-flux relation of the form,

$$j_{g\ell} = \langle\alpha\rangle(1-\langle\alpha\rangle)u_{R_o} = u_\infty\langle\alpha\rangle(1-\langle\alpha\rangle)^n \tag{52}$$

Thus, Eqs. 50–52 yield,

$$A^*_+ = 1 - n\langle\alpha\rangle \equiv 1 - n\alpha_o \tag{53}$$

Interestingly, this is exactly the same form as given in Eq. 42.

The value of the drift-flux parameter n depends on the flow conditions. For example, in steady, bubbly two-phase flow Eqs. 2 and 5 yield:

$$u_{R_o} = \left[\frac{4}{3}\frac{g(\rho_\ell-\rho_g)(1-\langle\alpha\rangle)D_b}{\rho_\ell C_D}\right]^{1/2} \tag{54}$$

For the distorted bubble regime Eq. 6 can be combined with Eq. 54 to yield,

$$u_{R_o} = 1.414\left[\frac{g(\rho_\ell-\rho_g)\sigma}{\rho_\ell^2}\right]^{1/4}(1-\langle\alpha\rangle)^{3/4}$$

That is,

$$u_{R_o} = u_\infty(1-\langle\alpha\rangle)^{3/4} \tag{55}$$

Hence Eqs. 52 and 55 imply $n = 7/4$ for distorted bubbly flow.

Finally, it should be noted that, using an entirely different analytical approach, Pauchon and Banerjee (1988) have deduced a result for the case of a constant interfacial drag coefficient, which yields $n = 3/2$. This result is consistent with the result proposed previously by Zuber and Hench (1962).

Thus we find that the void wave celerity given by a drift-flux model (which is based entirely on steady-state considerations) is closely linked, via the interfacial drag law, to the corresponding linear dispersion results of the two-fluid model, which is valid for low frequencies. This clearly shows the importance of interfacial drag on void wave propagation phenomena. Moreover, it implies that a great deal of physics associated with interfacial and wall momentum transfer is implicit in the empirical drift-flux parameter, n.

It appears that the linear dispersion relation of an appropriate two-fluid model is capable of predicting small-amplitude void wave propagation phenomena. In contrast, the void eigenvalues generally underpredict the wave speed of such data since these results imply zero interfacial drag, among other things. Moreover, it has also been shown that kinematic drift-flux models of void wave propagation are closely linked to the dispersion relation in which the corresponding interfacial drag law is used.

It can be noted in Figure 4 that the eigenvalues from Eqs. 45–46 show a strong sensitivity to C_{vm} and models for τ_{ℓ_i}. In particular, the domain of hyperbolicity of the two-fluid model is reduced when C_{vm} is greater than 0.5 and increased when it is less.

Moreover, including the interfacial shear stress, τ_{ℓ_i}, also reduces the domain of hyperbolicity. Indeed, a significant change can be noted when $C_{vm} \leq 0.5$. It is also interesting to note that for $C_{vm} < 0.5$, the lower branch of λ^* can be negative (i.e., r_- is less than $\langle u_\ell \rangle_{\ell o}$).

In addition, we note increasing values for λ^* as the void fraction approaches unity in Figure 4. This occurs because the primary contribution to the liquid pressure gradient is the hydrostatic head due to the mixture density. Thus, the relative velocity, $u_R = \langle u_g \rangle_g - \langle u_\ell \rangle_\ell$, approaches zero as the mixture density approaches that of the gas phase (i.e., bubble buoyancy goes to zero). This result is somewhat artificial since the bubbly flow drag law used in the eigenvalue predictions shown in Figure 4 is not appropriate for very high void fractions, nor are some of the other closure laws that have been used. While the same comments apply, this behavior was not seen in the model of Pauchon and Banerjee (1988) since no explicit expression for relative velocity was included.

Nonlinear Analysis of Void Wave Propagation

While linear analysis is important, it is clear that the propagation of finite-amplitude void waves cannot be modeled adequately using linear theory. Thus, in this part of the paper the propagation of finite-amplitude void waves will investigated theoretically.

The two-fluid model can be recast into a moving coordinate system using a Galilean transformation. It will be shown that solutions for nonlinear void wave profiles include solitons, shocks and rarefactions.

If we introduce a new coordinate system at celerity C_s, we obtain the Galilean relationship between the physical and the moving coordinate variables as,

$$\zeta = z - C_s t \tag{56}$$

Thus, Eqs. 1 and 2 can be rewritten in the Lagrangian (i.e., moving) coordinate system as,

$$(\langle u_k \rangle_k - C_s) \frac{d\langle \alpha_k \rangle}{d\zeta} + \langle \alpha_k \rangle \frac{d\langle u_k \rangle_k}{d\zeta} = 0 \tag{57}$$

$$\rho_k(\langle u_k \rangle_k - C_s) \frac{d\langle u_k \rangle_k}{d\zeta} = -\frac{dp_k}{d\zeta} + \frac{\Delta p_{ki}}{\langle \alpha_k \rangle} \frac{d\langle \alpha_k \rangle}{d\zeta} - \frac{\tau_{ki}}{\langle \alpha_k \rangle} \frac{d\langle \alpha_k \rangle}{d\zeta} + \frac{1}{\langle \alpha_k \rangle} \frac{d}{d\zeta} (\langle \alpha_k \rangle \tau^T_{zz_k}) - \rho_k g \cos\theta + \frac{M_{ki}}{\langle \alpha_k \rangle} - \frac{\tau_{kw}}{\langle \alpha_k \rangle} \frac{4}{D_H} \tag{58}$$

where we seek only steady solutions, and thus all time derivatives in the Lagrangian coordinate system have been set to zero. If we substract Eq. 58 for the gas phase from that for the liquid phase, and eliminate the phasic velocities using Eq. 57, we obtain:

$$\left[\rho_\ell \frac{(C_s - \langle u_\ell \rangle_\ell)^2}{(1-\langle \alpha \rangle)} + \rho_g \frac{(C_s - \langle u_g \rangle_g)^2}{\langle \alpha \rangle} + \frac{\Delta p_{\ell_i} - \tau_{\ell_i} + \tau^T_{zz_\ell}}{(1-\langle \alpha \rangle)} + \frac{\Delta p_{g_i} - \tau_{g_i} + \tau^T_{zz_g}}{\langle \alpha \rangle}\right] \frac{d\langle \alpha \rangle}{d\zeta} = -\frac{d}{d\zeta}(p_\ell - p_g - \tau^T_{zz_\ell} + \tau^T_{zz_g}) - (\rho_\ell - \rho_g) g \cos\theta + \frac{M_{\ell_i}}{(1-\langle \alpha \rangle)} - \frac{M_{g_i}}{\langle \alpha \rangle} - \frac{4}{D_H}\left[\frac{\tau_{\ell w}}{(1-\langle \alpha \rangle)} - \frac{\tau_{gw}}{\langle \alpha \rangle}\right] \tag{59}$$

where, $\langle \alpha \rangle \triangleq \langle \alpha_g \rangle = (1 - \langle \alpha_\ell \rangle)$.

Using Eqs. 7, 9, and 11, the two-phase interfacial momentum transfer in the moving coordinate system is:

$$M_{\ell_i} = -M_{g_i} = \langle \alpha \rangle \rho_\ell \left\{ \frac{f_i}{2D_H} (\langle u_g \rangle_g - \langle u_\ell \rangle_\ell) \mid \langle u_g \rangle_g - \langle u_\ell \rangle_\ell \mid - C_{vm} \left[\frac{(C_s - \langle u_g \rangle_g)^2}{\langle \alpha \rangle} + \frac{(C_s - \langle u_\ell \rangle_\ell)^2}{(1-\langle \alpha \rangle)} \right] \frac{d\langle \alpha \rangle}{d\zeta} \right\} \tag{60}$$

Inserting the closure laws, Eq. 60 and Eqs. 12–16, we obtain a single equation that quantifies the void fraction gradient in the moving coordinate system:

$$H(\langle \alpha \rangle, \langle u_\ell \rangle_\ell, \langle u_g \rangle_g, C_s) \frac{d\langle \alpha \rangle}{d\zeta} = G(\langle \alpha \rangle, \langle u_\ell \rangle_\ell, \langle u_g \rangle_g, C_s) \tag{61}$$

where

$$H(\langle \alpha \rangle, \langle u_\ell \rangle_\ell, \langle u_g \rangle_g, C_s) = \frac{[(1-\langle \alpha \rangle) + C_{vm}]}{(1-\langle \alpha \rangle)^2}(C_s - \langle u_\ell \rangle_\ell)^2 + \frac{[\rho_g^*(1-\langle \alpha \rangle) + C_{vm}]}{\langle \alpha \rangle (1-\langle \alpha \rangle)}(C_s - \langle u_g \rangle_g)^2 + 2(\langle u_g \rangle_g - \langle u_\ell \rangle_\ell)(\eta + k\langle \alpha \rangle)\left[\frac{C_s - \langle u_\ell \rangle_\ell}{(1-\langle \alpha \rangle)} + \frac{C_s - \langle u_g \rangle_g}{\langle \alpha \rangle}\right] + (\langle u_g \rangle_g - \langle u_\ell \rangle_\ell)^2 \left[k - \frac{\eta}{(1-\langle \alpha \rangle)}\right] \tag{62a}$$

$$G(\langle \alpha \rangle, \langle u_\ell \rangle_\ell, \langle u_g \rangle_g, C_s) = \frac{1}{2(1-\langle \alpha \rangle)D_H}[f_i(\langle u_g \rangle_g - \langle u_\ell \rangle_\ell)^2 - f_w \langle u_\ell \rangle_\ell^2] - (1-\rho_g^*) g \cos\theta \tag{62b}$$

and

$$\rho_g^* \triangleq \rho_g / \rho_\ell \tag{62c}$$

Characteristics, shocks, and kinematic wave speeds

It is interesting to note that the two-phase system's characteristics (eigenvalues) satisfy the following equation:

$$H(\langle \alpha \rangle, \langle u_\ell \rangle_\ell, \langle u_g \rangle_g, C_s^\infty) = 0 \tag{63}$$

Solving Eq. 63 for high frequency limit of the void wave celerity, C_s^∞, relative to the liquid-phase velocity, we again obtain the dimensionless characteristics as,

$$\lambda_{\pm}^{*} \triangleq \frac{C_s^{\infty} - u_\ell}{u_g - u_\ell} = V^* \pm \sqrt{v^*/\tau^*} \tag{64}$$

where, V^*, v^*, and τ^* have been previously defined in Eqs. 46.

The characteristics given by Eqs. 64 are the same as those in Eqs. 45, and reduce to those obtained by Pauchon and Banerjee (1986) if we let $C_{vm} = 1/2$, $\eta = 1/4$, $k = 0$, and $\rho_g^* = 0$.

If we assume that $H(\langle\alpha\rangle, \langle u_\ell\rangle_\ell, \langle u_g\rangle_g, C_s) \neq 0$ in Eq. 61, the void fraction gradient vanishes when

$$G(\langle\alpha\rangle, \langle u_\ell\rangle_\ell, \langle u_g\rangle_g, C_s) = 0 \tag{65}$$

Thus, the roots that satisfy Eq. 65 can be recognized as the steady states.

To identify the steady states given by Eq. 65, we must consider phasic continuity. If we add Eqs. 57 for each phase, we obtain,

$$\frac{d}{d\zeta}[\langle\alpha\rangle\langle u_g\rangle_g + (1-\langle\alpha\rangle)\langle u_\ell\rangle_\ell] = 0 \tag{66}$$

Integration of Eq. 66 directly yields the result that the total volumetric flux (j) is a conserved quantity in the $\zeta-\alpha$ plane:

$$j = \langle\alpha\rangle\langle u_g\rangle_g + (1-\langle\alpha\rangle)\langle u_\ell\rangle_\ell = \text{ constant} \tag{67}$$

We may obtain another conserved quantity, K, by noting that C_s is a constant, and integrating Eq. 57 for the liquid phase to obtain,

$$\langle\alpha\rangle C_s + (1-\langle\alpha\rangle)\langle u_\ell\rangle_\ell = K \tag{68}$$

Using Eqs. 67 and 68, we obtain the phasic velocities in terms of the void fractions and the conserved quantities:

$$\langle u_\ell\rangle_\ell = \frac{K - \langle\alpha\rangle C_s}{(1-\langle\alpha\rangle)} \tag{69a}$$

$$\langle u_g\rangle_g = C_s + \frac{(j-K)}{\langle\alpha\rangle} \tag{69b}$$

Inserting Eqs. 69 into Eq. 62b, we obtain:

$$G(\langle\alpha\rangle) = \frac{1}{2(1-\langle\alpha\rangle)D_H}\left\{f_i(\langle\alpha\rangle)\left[\frac{C_s-K}{(1-\langle\alpha\rangle)} + \frac{j-K}{\langle\alpha\rangle}\right]^2 - f_w\left[\frac{K-\langle\alpha\rangle C_s}{(1-\langle\alpha\rangle)}\right]^2\right\} - (1-\rho_g^*)g\cos\theta \tag{70}$$

Unfortunately, an analytic expression for the zeros of $G(\langle\alpha\rangle)$ is not possible. However, it has been found numerically that $G(\langle\alpha\rangle)$ has two zeros within the range of void fraction ($\langle\alpha\rangle$) from zero to unity, for all plausible values of j, K, C_s, and interfacial drag laws We designate these two zeroes α_1 and α_2.

Since j and K have been found to be conserved quantities we have, from Eqs. 67 and 68,

$$\alpha_1\langle u_g\rangle_{g_1} + (1-\alpha_1)\langle u_\ell\rangle_{\ell_1} = \alpha_2\langle u_g\rangle_{g_2} + (1-\alpha_2)\langle u_\ell\rangle_{\ell_2} \tag{71a}$$

$$\alpha_1 C_s + (1-\alpha_1)\langle u_\ell\rangle_{\ell_1} = \alpha_2 C_s + (1-\alpha_2)\langle u_\ell\rangle_{\ell_2} \tag{71b}$$

Solving Eq. 71b for C_s, we obtain:

$$C_s = \frac{(1-\alpha_1)\langle u_\ell\rangle_{\ell_1} - (1-\alpha_2)\langle u_\ell\rangle_{\ell_2}}{(\alpha_2-\alpha_1)} = \frac{j_{\ell_1} - j_{\ell_2}}{(\alpha_2-\alpha_1)} \tag{72}$$

It is interesting to note that the celerity given by Eq. 72 is the same as the continuity shock speed derived by Wallis (1969). Also, if we neglect wall friction, the shock speed referenced to the liquid-phase velocity can be found from Eqs. 70, 71a, and 72 as:

$$\frac{C_s - \langle u_\ell\rangle_{\ell_1}}{\langle u_g\rangle_{g_2} - \langle u_\ell\rangle_{\ell_1}} = \frac{(1-\alpha_2)}{(\alpha_2-\alpha_1)}\left[\alpha_2\sqrt{\frac{(1-\alpha_2)f_i(\alpha_1)}{(1-\alpha_1)f_i(\alpha_2)}} - \alpha_1\right] \tag{73}$$

Thus, Eq. 73 can be used to determine the shock speed C_s when a step change of the void fraction (e.g., from α_1 to α_2) is specified.

As a special case, the linear kinematic wave speed can be found from Eq. 73 when the void fraction change is small enough. That is,

$$A^*(\alpha_1) = \lim_{\alpha_2\to\alpha_1}\frac{(C_s - \langle u_\ell\rangle_{\ell_1})}{(\langle u_g\rangle_{g_1} - \langle u_\ell\rangle_{\ell_1})} = 1 - \frac{3}{2}\alpha_1 - \frac{\alpha_1(1-\alpha_1)}{2f_i(\alpha_1)}\left.\frac{df_i}{d\alpha}\right|_{\alpha_1} \tag{74}$$

Interestingly, this is the same result as given by Eqs. 42 and 43 for the special case of no wall shear and an f_i that is only a function of α.

Nonlinear void wave profiles

Phasic velocities in Eqs. 62 can be eliminated by using Eqs. 69. Therefore, we may obtain another form of Eq. 61 in which void fraction is the only dependent variable:

$$H(\langle\alpha\rangle)\frac{d\langle\alpha\rangle}{d\zeta} = G(\langle\alpha\rangle) \tag{75}$$

where, $H(\langle\alpha\rangle)$ can be obtained by inserting Eqs. 69 into Eq. 62a and $G(\langle\alpha\rangle)$ is given by Eq. 70.

Integrating Eq. 75 by separation of variables, we obtain an implicit expression for the void fraction profile in the $\zeta-\alpha$ plane:

$$\zeta = \int_{\langle\bar{\alpha}\rangle}^{\langle\alpha\rangle}\frac{H(\alpha')}{G(\alpha')}d\alpha' \tag{76}$$

where

$$\bar{\alpha}=(\alpha_1+\alpha_2)/2$$

$$\alpha_1<(\langle\alpha\rangle)<\alpha_2$$

and ζ is taken so that, $\zeta = 0$ at $\langle\alpha\rangle = \bar{\alpha}$.

Thus, the void fraction profile determined by Eq. 76 propagates at celerity C_s, given by Eqs. 73 or 78 when the void fraction is changed from α_1 to α_2 (or, from α_2 to α_1) without a variation in the total volumetric flux, j.

The kinematic wave speed is the first-order celerity, which controls the propagation of void fraction disturbances for nondispersive conditions (Park et al., 1990). As seen in Eq. 74, the kinematic wave speed depends on the interfacial friction factor. As shown in Figure 5, when we plot the kinematic wave speeds along with the characteristics, we find that a distorted bubble drag law (Harmathy, 1960), $n = 1.75$, yields unstable kinematic wave propagation based upon the linear stability criteria given by Whitham (1974), $\lambda_-^* < A^* < \lambda_+^*$. However, the kinematic wave is stabilized when an undistorted drag law (Ishii (Ishii and Mishima, 1984), $n = 2.5$, is used (Park et al., 1990). Some related properties between the stability of the kinematic wave and the nonlinear void wave are discussed later.

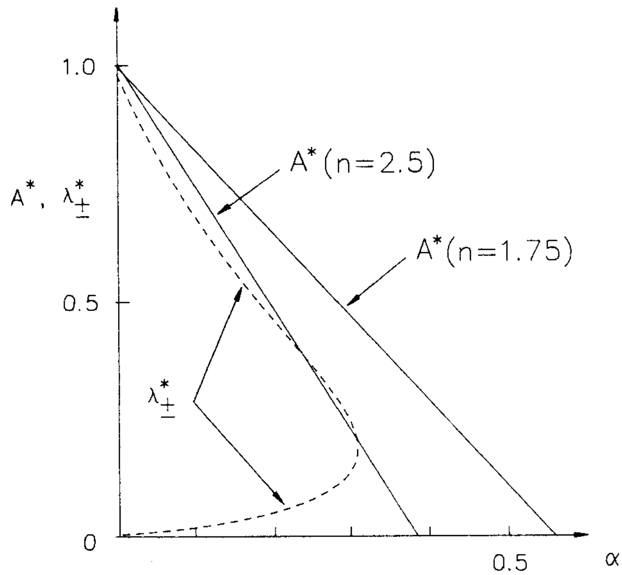

Figure 5. Kinematic wave speeds and characteristics.
$C_{vm} = 0.5$; $\eta = 0.25$; $k = 0.2$; $\rho_g^* = 0$; $\tau_{Lw}^* = 0$; $A^* = 1 - n\alpha$

Nonlinear void waves and their stability

To determine the nonlinear void wave profile using Eq. 76, we need the conserved quantities, j and K, and the speed of propagation, C_s, when the void fractions at the initial and the final states are specified. Since the total volumetric flux is normally known, K and C_s remain to be determined. These quantities can be obtained if we obtain the steady states, by solving $G(\alpha_1) = G(\alpha_2) = 0$ simultaneously, resulting in:

$$K=j+\sqrt{2gD_H\cos\theta(1-\rho_g^*)}\times\frac{\left[(1-\alpha_1)\sqrt{\dfrac{1-\alpha_1}{f_i(\alpha_1)}}-(1-\alpha_2)\sqrt{\dfrac{1-\alpha_2}{f_i(\alpha_2)}}\right]}{\left[\dfrac{1-\alpha_2}{\alpha_2}-\dfrac{1-\alpha_2}{\alpha_1}\right]} \qquad (77)$$

$$C_s=j+\sqrt{2gD_H\cos\theta(1-\rho_g^*)}\times\frac{\left[\dfrac{(1-\alpha_1)}{\alpha_2}\sqrt{\dfrac{1-\alpha_1}{f_i(\alpha_1)}}-\dfrac{(1-\alpha_2)}{\alpha_1}\sqrt{\dfrac{1-\alpha_2}{f_i(\alpha_2)}}\right]}{\left[\dfrac{1-\alpha_2}{\alpha_2}-\dfrac{1-\alpha_2}{\alpha_1}\right]} \qquad (78)$$

Before proceeding further, it should be noted that the nonlinear void wave profile breaks (i.e., the solution is multivalued in the $\zeta-\langle\alpha\rangle$ plane) when,

$$\alpha_2<\alpha_{o1},\ \alpha_{o2}\ldots<\alpha_1 \qquad (79)$$

where the eigenvalues are given by: $H(\alpha_{o1}) = H(\alpha_{o2}) = \ldots = 0$.

Possible nonlinear void wave profiles, which depend on the integrand of Eq. 76, are shown in Figure 6. When the zeroes of $H(\langle\alpha\rangle)$ satisfy Eq. 79, the void wave profile breaks as type B, C, E, or F shocks. Wave breaking occurs when C_s is between the larger characteristic speed of the initial state and that of the final state (Whitmam, 1974), that is,

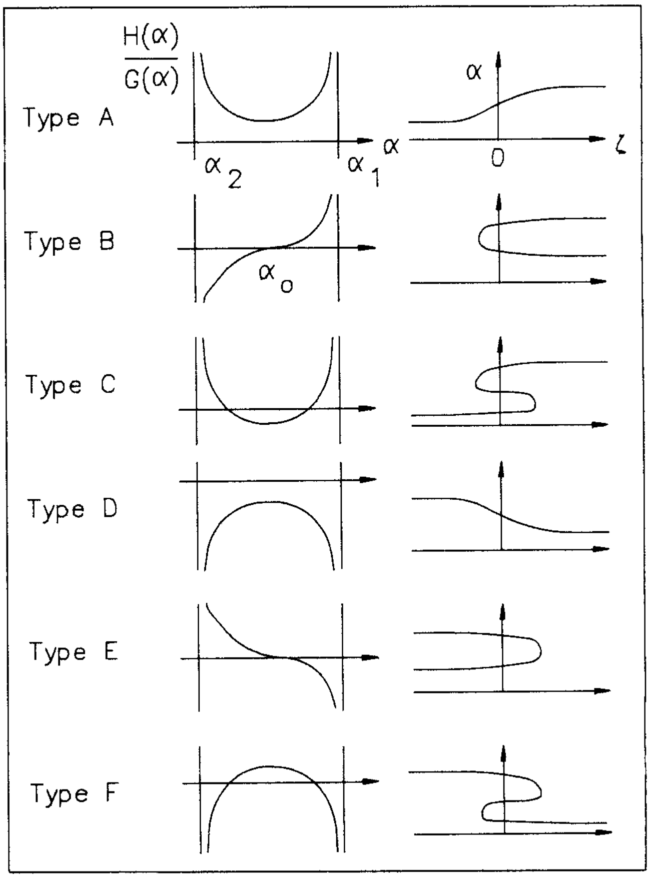

Figure 6. Types of nonlinear void wave profiles.

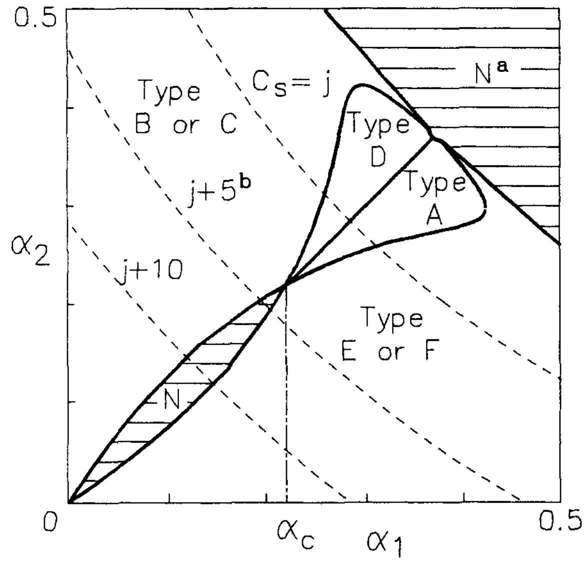

Figure 7. Different types of nonlinear void waves.
$C_{vm} = 0.5$; $\eta = 0.25$; $k = 0.2$; $\rho_g^* = 0$; $n = 2.5$
a. No solution is possible
b. All units are in cm/s

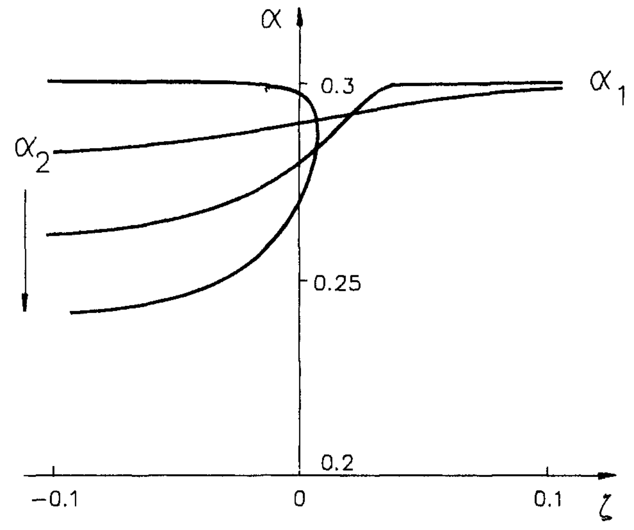

Figure 8. Breaking of void waves.
$C_{vm} = 0.5$; $\eta = 0.25$; $k = 0.2$; $\rho_g^* = 0$; $n = 2.5$

$$[\lambda_+^*(\langle u_g\rangle_g - \langle u_\ell\rangle_\ell) + \langle u_\ell\rangle_\ell]_1 < C_s < [\lambda_+^*(\langle u_g\rangle_g - \langle u_\ell\rangle_\ell) + \langle u_\ell\rangle_\ell]_2 \quad (80)$$

when $\alpha_1 > \alpha_2$. If we rearrange Eq. 80 by using Eqs. 69, 77 and 78, we obtain the condition for nonlinear void wave breaking (i.e., shockformation) as,

$$\frac{\lambda_+^*(\alpha_2)}{1-\lambda_+^*(\alpha_2)}(1-\alpha_2)\alpha_1 < \frac{(\alpha_2-\alpha_1)}{1-\sqrt{\dfrac{f_i(\alpha_1)(1-\alpha_2)}{f_i(\alpha_2)(1-\alpha_1)}\,\dfrac{1-\alpha_2}{1-\alpha_1}}} < \frac{\lambda_+^*(\alpha_1)}{1-\lambda_+^*(\alpha_1)}(1-\alpha_1)\alpha_2 \quad (81)$$

Based upon the above wave-breaking criteria, different types of void wave profiles are categorized in Figure 7. As can be seen, C_s decreases as α_2 increases for a specified initial state (α_1). This result can be understood easily if we realize that these shock (or rarefaction) solutions are based on a kinematic condition that implies a reduction in wave speed with void fraction (note that $dA^*/d\alpha < 0$ in Figure 5).

If we consider the region $\alpha_1 > \alpha_2$ and $\alpha_1 > \alpha_c$ in Figure 7, we see that solitons—that is, the smooth void wave profiles (type A or D)—break when the void fraction change, $\alpha_1 - \alpha_2$, is large. The evolving void wave profiles for different values of the void fraction change are shown in Figure 8.

In the region $\alpha_1 < \alpha_c$ in Figure 7, there exists a region where small-amplitude void wave solutions are not possible based on the present techniques. Interestingly, α_c is the point where the kinematic wave speed and the faster characteristic coalesce in Figure 5. Since, based upon the linear stability criteria, $\lambda_-^* < A^* < \lambda_+^*$, the linear void wave is unstable where $0 < \alpha < \alpha_c$, we find this result is more general. It should also be noted that the nonlinear void wave solutions are also not possible in the region where the initial and the final void fractions are large.

None of the solutions in the region, $\alpha_1 < \alpha_2$, are stable (Whitman, 1974) since the upstream celerity (i.e., the kinematic wave speed, A^*, for $\alpha = \alpha_1$) is smaller than that for the downstream conditions (A^* for $\langle\alpha\rangle = \alpha_2$). Indeed the solutions are rarefractions, such that if void waves are generated by increasing the void fraction, they will decay out.

As can be seen in Figure 9, if we use a distorted bubble drag model (e.g., $n = 1.75$), smooth wave profile solutions (types A or D) are not possible. This result suggests that the increased interfacial drag associated with bubble distortion promotes

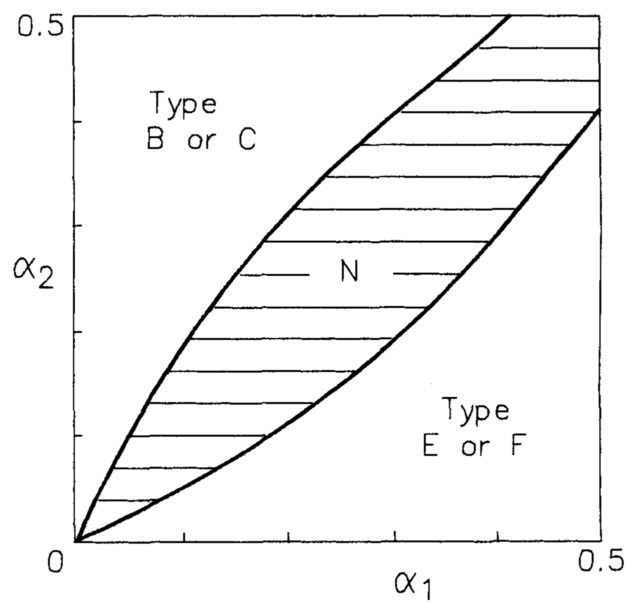

Figure 9. Different types of void waves with distorted bubble drag models.
$C_{vm} = 0.5$; $\eta = 0.25$; $k = 0.2$; $\rho_g^* = 0$; $n = 1.75$

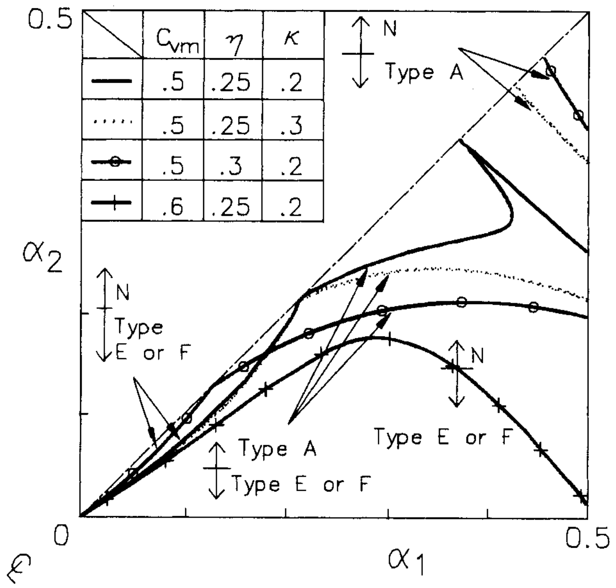

Figure 10. Dependency of void wave types on two-fluid constitutive relations.
$\rho_g^* = 0; n = 2.5$

discontinuity in the two-fluid variables before and after the transition.

The effects of the virtual mass force, the interfacial pressure difference and the bubble-induced Reynolds stress are shown in Figure 10. From these results, we see that the virtual mass force is crucial in determining the behavior of nonlinear void waves. In particular, the smooth wave profiles in the high void fraction region totally disappear when the virtual volume coefficient is increased from 0.5 to 0.6. In contrast, increasing the interfacial pressure difference and/or the Reynolds stress increases regions A and D monotonically, which means that these effects reduce the void fraction gradient between the two steady states.

Conclusions

It has been shown that the linear dispersion model appears to be able to quantify void wave dispersion. Void wave dispersion is pronounced for large values of the relaxation time, T, which is determined by the Froude number, the virtual mass coefficient, and the void fraction. Since the relaxation time is small for large values of relative velocity (where the Froude number is small), void waves in a stagnant pool of liquid can successfully be described by a kinematic wave model. However, since relaxation time increases as relative velocity decreases (i.e., the Froude number becomes large), the void waves become dispersive when slip is reduced. The virtual mass effect also promotes void wave dispersion since relaxation time is increased as the virtual volume coefficient (C_{vm}) is increased.

It was found that nonlinear void wave speed increases as the amplitude of the wave increases. Moreover, the nonlinear void wave speed reduces to the linear void wave speed for small amplitudes.

Different types of void wave profiles are predicted, in particular, solitons and shocks. Smooth time-invariant void wave profiles (i.e., solitons) are possible only when the void fraction is relatively large, and void waves generated by a large step change in the void fraction eventually break (i.e., strong shocks occur). It is significant to note that among the two-fluid closure parameters studied, the virtual volume coefficient (C_{vm}) most strongly affects the discontinuity in the two-fluid variables.

Unfortunately, the existing void wave propagation data exhibit significant scatter and do not include the measurement of the attention coefficient. Furthermore, the existing data for C_α^+ are not accompanied by sufficient supporting information on the flow state, or the nature of the void perturbation (frequency, amplitude, etc.), thus, complete two-fluid model assessment is not possible at this time. Nevertheless, it appears that carefully taken void wave propagation data can be a powerful tool for assessing two-fluid interfacial momentum transfer laws due to the relatively large sensitivity in the void wave speeds, $C_\alpha^\pm$, and wave form to the interfacial closure laws. Indeed, it appears that comparison between these data and the analysis of void wave phenomena is very valuable for the assessment of two-fluid models.

Acknowledgment

This article is based on the Kern Award Lecture. The author wishes to acknowledge the support given to this work by the USDOE-BE, and the assistance of Prof. D. A. Drew and Mr. J.-W. Park in the conduct of this research.

Notation

a = acceleration
a_{vm} = virtual mass acceleration
C = speed of propagation (celerity)
C_{vm} = virtual volume coefficient
D = diameter
$D_k(\ )/Dt$ = material derivative, $[\partial(\ )/\partial t] + u_k[\partial(\ )/\partial z]$
f = frequency; friction factor
F = force
g = gravitational acceleration
j_k = superficial velocity of phase k
$j_{g\ell}$ = drift flux
k = wave number
M_{k_i} = interfacial momentum transfer
n = drift-flux parameter
p = pressure
r = eigenvalue
R = radius
T = relaxation time
t = time
u = velocity
z = axial location

Greek letters

α = void fraction
$\delta(\cdot)$ = perturbed quantity
λ = wavelength
μ = dynamic viscosity
ω = angular frequency
ρ = density
κ = Reynolds stress parameter
Ψ = state vector
σ = surface tension
θ = angle of inclination of flow from vertical
τ = stress
υ = kinematic viscosity
ξ = interfacial pressure distribution parameter

Subscripts

b = bubble
2ϕ = two-phase
1ϕ = one-phase
g = gas
H = hydraulic
i = interfacial
k = phase indicator (g = gas, ℓ = liquid)
ℓ = liquid
o = equilibrium (steady-state) value
vm = virtual mass
w = wall
∞ = terminal rise (velocity)

Symbols

$()^T$ = transpose of a vector matrix
∇ = gradient
$\partial()/\partial()$ = partial derivative
$d()/d()$ = total derivative
$\langle\ \rangle$ = cross-sectional average

Literature Cited

Biesheuvel, A., and L. van Wijngaarden, "Two-Phase Flow Equations for a Dilute Dispersion of Gas Bubbles in Liquid," *J. Fluid Mech.*, **168**, 301 (1984).

Bouré, J. A., "Properties of Kinematic Waves in Two-Phase Pipe Flows; Consequences on the Modeling Strategy," *Proc. Eur. Two-Phase Flow Group Meet., Brussels* (1988).

Cheng, L-Y., D. A. Drew, and R. T., Lahey, Jr., "An Analysis of Wave Propagation in Bubbly Two-Component Two-Phase Flows," *J. Heat Transfer*, **107**, 402 (1985).

Drew, D. A., and L. T. Lahey, Jr., "The Virtual Mass and Lift Force on a Sphere in Rotating and Straining Inviscid Flow," *Int. J. Multiph. Flow*, **13**(1) (1987).

Harmathy, T. Z., "Velocity of Large Drops and Bubbles in Media of Infinite or Restricted Extent," *AIChE J.*, **6**(2), 281 (1960).

Ishii, M., and K. Mishima, "Two-Fluid Model and Hydrodynamic Constitutive Relations," *Nuclear Eng. Des.*, **82**, 107 (1984).

Ishii, M., and N. Zuber, "Relative Motion and Interfacial Drag Coefficent in Dispersed Two-Phase Flow of Bubbles, Drops and Particles," Paper 56a, AIChE 71st Ann. Meet., Miami (1978).

Lahey, R. T., Jr., and D. A. Drew, "The Three-Dimensional Time- and Volume-Averaged Conservation Equations of Two-Phase Flows," *Adv. Nucl. Sci. Technol.*, **20**, 1 (1989).

Lahey, R. T., Jr., and M. Z. Podowski, "On the Analysis of Instabilities in Two-Phase Flow," *Multiph. Sci. Technol.*, **4**, 183(1989).

Nigmatulin, R. I., "Spatial Averaging in the Mechanics of Heterogeneous and Dispersed Systems," *J. Multiph. Flow*, **5** (1979).

Park, J-W., D. A. Drew, and R. T. Lahey, Jr., and "Void Wave Dispersion in Bubbly Flows," *Nucl. Eng. Des.*, **121**, 1 (1990).

Pauchon, C., and S. Banerjee, "Interphase Momentum Effects in the Averaged Multifield Model, I: Void Propagation in Bubbly Flows," *Int. J. Multiph. Flow*, **12**(4), 559 (1986).

Pauchon, C., and S. Banerjee, "Interphase Momentum Effects in the Averaged Multifield Model: II. Kinematic Waves and Interfacial Drag in Bubbly Flows," *Int. J. Multiph. Flow*, **14**(3), 253 (1988).

Ruggles, A. E., R. T. Lahey, Jr., and D. A. Drew, "An Analysis of Void Wave Propagation in Bubbly Flows," *Proc. 15th Miami Intl. Symp. Multiphase Transport and Particulate Phenomena*, (1988).

Saiz-Jabardo, J. M., and J. A.Bouré, "Experiments on Void Fraction Waves," *Int. J. Multiph. Flow*, **15**(4), 483 (1989).

Stuhmiller, J. H., "The Influence of Interfacial Pressure Forces on the Character of Two-Phase Flow Model Equations," *J. Multiph. Flow*, **3**, 551 (1977).

Tournaire, A., "Détection et Études des Ondes de Taux Vide en Écoulement Diphasique a Bulles Jusqu'a la Transition Bulles-Bouchons," Docteur-Ingénieur Thesis, L'Université Scientifique et Médicale et L'Institut National Polytechnique de Grenoble (1987).

Wallis, G. B., *One-Dimensional Two-Phase Flows*, McGraw-Hill, New York (1969).

Whitham, G. B., *Linear and Nonlinear Waves*, Wiley, New York (1974).

Zuber, N., and J. Hench, "Steady-State and Transient Void Fraction for Bubbling Systems and Their Operating Limit: 1. Steady-State Operation," General Electric Report No. 62 GL 100 (1962).

Manuscript received Aug. 9, 1990, and revision received Nov. 26, 1990.